ARTICLE NO. 78-1307R

Optimizing the Gains of the Baro-Inertial Vertical Channel

William S. Widnall*
Massachusetts Institute of Technology, Cambridge, Mass.
and
Prasun K. Sinha†
Intermetrics, Inc., Cambridge, Mass.

The selection of the three gains in the baro-inertial vertical channel has been formulated as a stochastic optimal control problem, where the objective is to minimize the mean-square error of the indicated vertical velocity. The optimal set of gains is surprisingly different from a conventional set of gains, and it provides a significant performance improvement. Sensitivity of the results to the statistical assumptions is explored. Approximate analytical formulas are presented giving the optimal gains and pole locations as a function of the assumed statistics of the sources of error. A time domain simulation also exhibits the performance improvement.

Introduction

THE first aircraft inertial navigation systems were primarily two-channel systems that provided horizontal navigation data.[1-3] Inertial navigators instrumenting three channels were introduced for missile navigation and guidance. In addition, the value of inertially derived vertical velocity was recognized in aircraft applications involving flight path angle determination and precision weapon delivery. It is well known that the altitude channel of a pure inertial navigation mechanization, in which gravity magnitude is computed as a function of the indicated altitude, is unstable.[4-6] Near the surface of the Earth, the time constant of this exponential instability is about 10 min. Hence, for typical cruise navigation durations, the vertical channel of a terrestrial inertial navigator must be stabilized by some external altitude reference.

The most commonly used external altitude reference in aircraft is a barometric altimeter. The optimal time-varying combination of the inertial and barometric data may be obtained using a Kalman filter.[7] However, in applications not demanding the minimum navigation errors or in which the computer capacity is severely limited, a simple mechanization is commonly used in which the difference between the indicated and barometric altitude is fed back through constant gains or simple transfer functions to stabilize the altitude navigation variables.[8] A typical set of constant-gain baro-inertial mechanization equations, which is analyzed in detail in this paper, is

$$\dot{h}=v_z-k_1(h-h_b) \tag{1a}$$

$$\dot{v}_z=f_z-g(h,L)+\text{Coriolis terms}-k_2(h-h_b)-\hat{\delta a} \tag{1b}$$

$$\dot{\hat{\delta a}}=k_3(h-h_b) \tag{1c}$$

where h is the indicated altitude, v_z is the indicated vertical velocity, $\hat{\delta a}$ is the computed vertical acceleration error, f_z is the measured vertical specific force, g is the magnitude of gravity computed as a function of indicated altitude and latitude, and k_1, k_2, k_3 are the loop gains. This third-order vertical channel mechanization is superior to a second-order mechanization, which omits the $\hat{\delta a}$ equation, because it has zero vertical velocity error due to any bias vertical acceleration error such as accelerometer bias or gravity computation error.

The Litton CAINS (Carrier Aircraft Inertial Navigation System) implements such a third-order baro-inertial vertical channel. In the CAINS, the three gains have been chosen so that the characteristic equation of the errors has a triple pole at the complex frequency $s=-1/\tau$, where τ is the desired time constant. For such a triple pole placement, it can be shown one chooses the gains to be

$$k_1=3/\tau \qquad k_2=3/\tau^2+2g/R \qquad k_3=1/\tau^3 \tag{2}$$

where R is the geocentric radius. In the CAINS, the time constant has been chosen to be $\tau=100$ s. We have no literature explaining the designer's choice of the triple pole and its location. Perhaps the triple pole configuration was arbitrarily selected to reduce the gain-setting problem from three parameters (k_1, k_2, k_3) to one parameter (τ). Speculating further, perhaps the time constant of 100 s was an order-of-magnitude choice, selected so as to be faster than the 571 s time constant of the pure-inertial vertical-channel instability yet slower than the typical barometric error fluctuations associated with short-term aircraft maneuvers. This choice would be expected to both stabilize the vertical channel and provide some smoothing of the barometric altimeter errors. Regardless of the reasoning, the CAINS has peformed well in its intended applications. We shall refer to the CAINS set of gains, given by Eq. (2) with $\tau=100$ s, as the baseline set.

Some applications have more demanding vertical velocity requirements than the CAINS requirements. In such applications it may be necessary to optimize the vertical channel gains to reduce the vertical velocity errors. One such application was the use of the Magnavox X-set GPS navigator in the demonstration of pinpoint bombing on a target whose absolute coordinates were known. The X-set GPS navigator includes a barometric-inertial navigation subsystem and a GPS X-set receiver whose outputs are combined by a Kalman filter. An error analysis by Ausman[9] predicted that the two largest contributions to bomb miss distance would be due to

Received June 26, 1978; presented as Paper 78-1307 at the AIAA Guidance and Control Conference, Palo Alto, Calif., Aug. 7-9, 1978; revision received July 3, 1979.

Index category: Guidance and Control.

*Associate Professor, Dept. of Aeronautics and Astronautics. Associate Fellow AIAA.

†Senior Engineer, Navigation and Analysis Dept.

the altitude navigation error and the vertical velocity navigation error at bomb release. Flying at 450 knots, at 5000-ft altitude above ground level, with a level release, and using low-drag bombs, Ausman indicated that the anticipated altitude and vertical velocity navigation errors of 19 m and 0.75 m/s would contribute 24 m and 17 m, respectively, to downrange bomb miss distance. The absolute altitude error of the integrated navigation system is caused by the bias-like errors in the GPS measurements. The choice of baro-inertial gains has little or no effect on the absolute altitude accuracy. However, the absolute vertical velocity errors are a noticeable function of both the GPS measurement errors and the baro-inertial errors. The integrated system vertical velocity errors can be reduced if first the baro-inertial vertical velocity errors are minimized.

There is no reason to assume that the triple pole gain set provides the best performance. Other pole placements might provide superior performance. To obtain new insights into the effect of the gains, we have formulated the vertical channel gain setting problem as a parameter optimization problem for the control of a stationary stochastic process. This paper presents the optimization problem formulation, computational results, analysis of the results, and a time-domain simulation of the performance with the recommended gains.

Before proceeding, we comment that any constant gain set (including our optimized set) will be less optimal than appropriate time-varying gains that take into account the nonstationary nature of the inertial and barometric altimeter errors. The optimal time-varying combination of the inertial and barometric data may be obtained using a Kalman filter. Of course it is also possible to select effective time-varying gains with non-Kalman approaches. One example of the use of time-varying gains is provided by Whalley.[10] Whalley points out the large error in barometric altitude when a supersonic aircraft passes through Mach 1 due to shock waves moving past the static pressure port. Whalley suggests eliminating this source of error by switching out the air data automatically from say Mach 0.95 to Mach 1.1. This could be mechanized by programming k_1, k_2, k_3 to be zero in this Mach interval.

Another example of the use of time-varying gains is provided by Ausman and associates.[11,12] They note that in subsonic flight the largest source of barometric altimeter error is often the scale factor error due to the atmosphere not having the standard-day temperature-vs-altitude profile. In climbs and dives the scale factor error induces significant vertical velocity error into a constant gain baro-inertial vertical channel. Ausman and associates designed and implemented vertical channel mechanizations that reduce the gains during climbs and dives, while observing the baro-bias shift due to scale factor error. The estimated baro-bias shift is automatically subtracted from the baro-inertial error feedback so that loop transients due to the scale factor error are minimized.

Also before proceeding, we comment that additional external data may be useful in reducing the effect of nonstandard-day temperature. Blanchard[13] proposes using in-flight measured temperature data, in place of the standard-day lapse-rate assumption, to relate more accurately pressure changes to altitude changes.

Formulation of the Gain-Optimization Problem

The error model for the vertical channel is shown in Fig. 1. The positive feedback with gain $2g/R$ is the destabilizing effect of normal gravity being calculated at the closed-loop altitude, which is in error by δh. The error state δa is a random walk modeling any bias or slowly varying error in the vertical acceleration due to accelerometer bias, gravity anomaly, or error in the Coriolis terms. The white noise w_{a2} into the integration provides the random walk. The white noise w_{a1} models short correlation time acceleration error, such as the effect during a short maneuver of vertical accelerometer scale

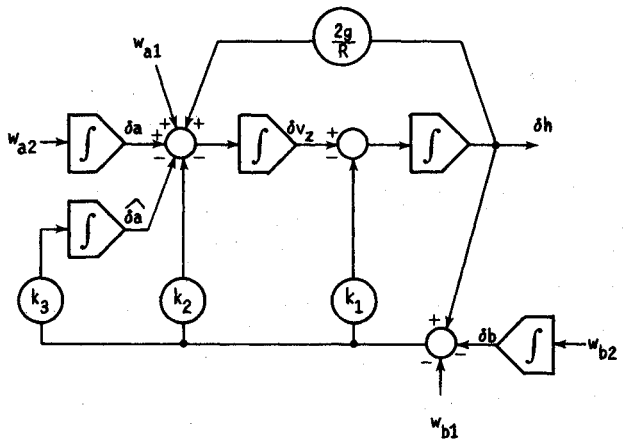

Fig. 1 Baro-inertial vertical channel error model.

factor error and input axis misalignment. The error state δb is a random walk modeling any bias or slowly varying error in the altitude indicated by the barometric altimeter. Physical error sources include zero setting error, static pressure measurement error, variation in the height of a constant pressure surface, and scale factor error due to nonstandard day temperature. The white noise w_{b2} into the integrator provides the random walk. The white noise w_{b1} models short correlation time altimeter error, such as due to changes in the angle of attack or sideslip angle during a maneuver, or due to altimeter quantization or other noise.

It is difficult to suggest appropriate values for the spectral densities of the four independent white noises in this stochastic model. Nevertheless, it must be done for the analysis to proceed. Table 1 shows the nominal values of the noise spectral densities that have been selected. These somewhat arbitrary numerical values have been arrived at by the following considerations.

For the short correlation time acceleration error, a typical amplitude could be 200 μg. This error could be caused by a vertical accelerometer input axis misalignment of 200 μ rad (41 arc-sec) together with a horizontal maneuver acceleration of one g. The typical duration of a horizontal maneuver is assumed to be of the order of 60 s. For a repeated series of random aircraft maneuvers, the autocorrelation function of the acceleration error would have area approximately

$$Q_{a1} = (200\times 10^{-6}\times 10\,\mathrm{ms}^{-2})^2\times(60\mathrm{s}) = 2.4\times 10^{-4}\,\mathrm{m^2 s^{-3}} \quad (3)$$

The area of the autocorrelation function equals the low-frequency value of the spectral density. For the white noise, whose autocorrelation function is a Dirac delta function with area Q_{a1}, the spectral density Q_{a1} applies at all frequencies. Of interest is the response of the vertical channel at frequencies lower than the higher frequencies of the short-correlation acceleration error. So the low-frequency density of Eq. (3) is used for the spectral density of the white noise.

Table 1 Nominal values of noise spectral densities

White noise for	Noise density symbol	Noise density value
Short correlation time acceleration error	Q_{a1}	$2.4\times 10^{-4}\,\mathrm{m^2\,s^{-3}}$
Acceleration error random walk	Q_{a2}	$1.0\times 10^{-9}\,\mathrm{m^2\,s^{-5}}$
Short correlation time altimeter error	Q_{b1}	$100\,\mathrm{m^2\,s}$
Altimeter error random walk	Q_{b2}	$100\,\mathrm{m^2\,s^{-1}}$

The acceleration error random walk models the slowly varying error due to accelerometer bias shifts, changes in the gravity anomaly, and changes in the error in the Coriolis terms. If over a period of 1000 s, the accelerometer bias were expected to shift 100 μg, the appropriate noise spectral density for the random walk is

$$Q_{a2} = (100\times 10^{-6}\times 10\,\mathrm{ms}^{-2})^2/(1000\,\mathrm{s}) = 1.0\times 10^{-9}\,\mathrm{m^2 s^{-5}} \tag{4}$$

For the short correlation time altimeter error, it is assumed that repeated random fluctuations of the order of 10 m may be present in the baro-indicated altitude, and that these errors persist for correlation times of the order of 1 s. To match the low-frequency spectral density of this error, the white noise error model should have density

$$Q_{b1} = (10\,\mathrm{m})^2\times(1\,\mathrm{s}) = 100\,\mathrm{m^2 s} \tag{5}$$

The altimeter error random walk models the slowly varying error due to: changes in the static pressure measurement error (due to speed changes), variations in the height of a constant pressure surface (the weather pattern of highs and lows), and scale factor error (related to nonstandard-day temperature and nonzero aircraft climb or descent rate). For an atmospheric scale factor error of 3% and an aircraft climb or descent rate of 33 m/s (6500 ft/min), the error rate of the baro-indicated altitude is 1.0 m/s. If the climb or descent continues for 100 s, the change in altimeter error will be 100 m. Assume that the aircraft trajectory is characterized by a random sequence of such climbs and descents. The appropriate noise spectral density for the random walk is then

$$Q_{b2} = (100\,\mathrm{m})^2/(100\,\mathrm{s}) = 100\,\mathrm{m^2 s^{-1}} \tag{6}$$

The mean-squared error of the indicated vertical velocity has been selected as an appropriate performance index. Note that with the random walk error models for acceleration error and for altimeter error, only the vertical velocity error has a stationary and finite mean-square value. All other error states have mean-square values that grow unbounded with time. Referring to Fig 1, $\delta\hat{a}$ tracks $\delta a + (2g/R)\delta h$ as this sum wanders off, and δh tracks δb as it wanders off.

The mean-squared vertical velocity error may be computed as an explicit function of the input noise spectral densities and of the loop gains. One first calculates four transfer functions $H_i(s)$ relating the vertical velocity error response to each independent white noise input. The power spectrum of the vertical velocity error is then

$$\Phi_{\delta v}(\omega) = \sum_{i=1}^{4} H_i(j\omega) H_i(-j\omega) Q_i \tag{7}$$

where Q_i is the spectral density of the ith white noise. The mean-square value of the vertical velocity error is the integral of the power spectrum

$$\overline{(\delta v)^2} = \sum_{i=1}^{4} \frac{Q_i}{2\pi j}\int_{-j\infty}^{j\infty} H_i(s) H_i(-s)\,ds \tag{8}$$

The four integrals are evaluated using an appropriate table of integrals.[14] The result is

$$\overline{(\delta v)^2} = \frac{(k_1^2 + k_2 - c)Q_{a1}}{2[k_1(k_2-c)-k_3]} + \frac{(k_3+k_1^3)Q_{a2}}{2k_3[k_1(k_2-c)-k_3]} + \frac{[k_2^2(k_2-c)+(k_3+ck_1)^2]Q_{b1}}{2[k_1(k_2-c)-k_3]} + \frac{[k_2^2 k_3 + (k_3+ck_1)^2 k_1]Q_{b2}}{2k_3[k_1(k_2-c)-k_3]} \tag{9}$$

where near the surface of the Earth $c = 2g/R = 3.07\times 10^{-6}\,\mathrm{s^{-2}}$. For the steady-state solution to exist and be equal to Eq. (9), the set of loop gains must yield a stable system. Therefore, the permissible values of the gains are in the regions defined by

$$k_1 > 0, \quad k_2 - c > 0, \quad k_3 > 0, \quad k_1(k_2-c) - k_3 > 0 \tag{10}$$

The explicit computation of the mean-squared vertical velocity error is used in a computer program that seeks a set of gain values that minimizes the mean-squared error. The pattern search algorithm of Hooke and Jeeves[15] has been utilized. The algorithm does not require explicit gradient information.

The natural frequencies (poles) of the closed-loop portion of the baro-inertial vertical channel are the three roots of the characteristic equation

$$s^3 + k_1 s^2 + (k_2 - c)s + k_3 = 0 \tag{11}$$

For a candidate set of gains, it is often of interest to inspect the locations of the three poles p_1, p_2, p_3. In such a case, the roots of the cubic Eq. (11) are computed according to the known formulas for those roots. When the time constant of a pole is mentioned, it is defined to be the inverse of the real part of the complex frequency of the pole.

Optimization Results

To provide a baseline design and performance against which to compare the optimized performance, the mean-squared velocity error is evaluated for the set of gains, Eq. (2), which place a triple pole at $\tau = 100$ s

$$k_1 = 3.0\times 10^{-2}\,\mathrm{s^{-1}} \qquad k_2 = 3.0307\times 10^{-4}\,\mathrm{s^{-2}}$$
$$k_3 = 1.0\times 10^{-6}\,\mathrm{s^{-3}} \tag{12}$$

The mean-squared velocity error, with the nominal (Table 1) values of noise spectral densities, is found to be

$$\overline{(\delta v)^2} = 0.818\,\mathrm{m^2 s^{-2}} = (0.904\,\mathrm{m/s})^2 \tag{13}$$

Using the Hooke and Jeeves pattern search procedure, the gains that minimize the mean-square velocity error, with the nominal noise densities, are found to be

$$k_1 = 1.003\,\mathrm{s^{-1}} \qquad k_2 = 4.17\times 10^{-3}\,\mathrm{s^{-2}}$$
$$k_3 = 4.39\times 10^{-6}\,\mathrm{s^{-3}} \tag{14}$$

The corresponding value of the mean-square velocity error is

$$\overline{(\delta v)^2} = 0.418\,\mathrm{m^2\,s^{-2}} = (0.647\,\mathrm{m/s})^2 \tag{15}$$

This is a significant performance improvement relative to the baseline case. The rms velocity error is 30% lower.

The three poles associated with the gain set, Eq. (14), are located at

$$p_1 = -0.998\,\mathrm{s^{-1}} \quad p_2, p_3 = -2.082\times 10^{-3} \pm j\,2.34\times 10^{-4}\,\mathrm{s^{-1}} \tag{16}$$

They have time constants of

$$\tau_1 = 1.002\,\mathrm{s} \qquad \tau_2, \tau_3 = 480.3\,\mathrm{s} \tag{17}$$

The optimized gains and resulting pole placements (and time constants) are radically different from the baseline triple pole set. One time constant is a factor of 100 faster; the other two time constants are a factor of 5 slower.

Table 2 Contributions to mean-square velocity error of nominal noise densities

Noise density	Mean-square velocity error, $(m/s)^2$ Triple pole, $\tau = 100$ s	Optimized set
Q_{a1}	0.018	0.0291
Q_{a2}	0.00175	0.0275
Q_{b1}	0.00018	0.00087
Q_{b2}	0.798	0.361
Total	$0.818 = (0.904)^2$	$0.418 = (0.647)^2$

The individual contributions of the various white noises to the mean-square velocity error are shown in Table 2, for the nominal values of the white noise spectral densities. The data of this table show that the mean-square velocity error is dominated by the altimeter error random walk (Q_{b2}), while the contribution of short correlation time altimeter error (Q_{b1}) is least.

To obtain further insight into the nature of the optimal solution and to exhibit the sensitivity of the optimal solution to the noise density assumptions, the optimal solution has been computed for various values of the noise spectral densities. Table 3 shows the results for four cases in which one of the noise densities is increased while holding the other three densities at their nominal (Table 1) values.

With the optimized gains being so different from the baseline gains, it is interesting to ask: for what set of input noise densities are the "triple pole" gains optimal? From Table 2, one notes that in the "triple pole" case, the contributions of the altimeter error noises to the mean-square velocity error would be more nearly equal if Q_{b1} were 10 times larger and Q_{b2} were 100 times smaller. The optimization program has been rerun with these altered values for noise density. The results are presented as the last case in Table 3. These results demonstrate that the baseline triple pole set is close to being an optimal set if the random walk component of the altimeter error is significantly smaller and if the short correlation time altimeter error is somewhat larger than the nominal assumed values.

Analysis of Results

In all cases presented in the previous section (except the greatly reduced Q_{b2} case) the dynamics of the optimal third-order vertical channel are that of a fast first-order loop nested inside a slower second-order system. From Table 3 it is clear that the fast pole frequency is simply related to the first gain

$$p_1 \approx -k_1 \tag{18}$$

With such a fast real pole, the characteristic equation of the third-order vertical channel can be factored as

$$(s+k_1)\left(s^2+\frac{k_2'}{k_1}s+\frac{k_3}{k_1}\right)\approx 0 \tag{19}$$

where

$$k_2' = k_2 - c \tag{20}$$

This can be shown by multiplying the two factors in Eq. (19) to obtain

$$s^3+\left(k_1+\frac{k_2'}{k_1}\right)s^2+\left(k_2'+\frac{k_3}{k_1}\right)s+k_3\approx 0 \tag{21}$$

The correct characteristic equation of the third-order vertical channel, Eq. (11), in terms of k_2' is

$$s^3+k_1s^2+k_2's+k_3=0 \tag{22}$$

Comparing Eqs. (21) and (22), it is clear that sufficient conditions for the factorization of Eq. (19) to be true are

$$k_2' \ll k_1^2 \tag{23}$$

$$k_3 \ll k_1k_2' \tag{24}$$

Inspecting the second-order factor of Eq. (19), one sees that the two slower poles are a function only of the two gain ratios k_2'/k_1 and k_3/k_1. The pole locations are

$$p_2,p_3 \approx \frac{-k_2'}{2k_1} \pm \sqrt{\left(\frac{k_2'}{2k_1}\right)^2-\frac{k_3}{k_1}} \tag{25}$$

Equation (25) gives good agreement with the values of poles and gains in the computed results (Table 3).

The optimized gain k_1 in the nominal noise density case has a very curious numerical value of unity. This provides a clue that there exists a very simple relationship between this gain

Table 3 Changes in optimal solution with altered noise densities

	Optimal gains: k_1, s^{-1}, k_2, s^{-2}, k_3, s^{-3}	Pole locations, s^{-1}	Time constants, s
Nominal case (Table 1 values)	1.003	-0.998	1.002
	4.17×10^{-3}	-2.082×10^{-3}	480.3
	4.39×10^{-6}	$\pm j\,2.34\times10^{-4}$	480.3
Increased Q_{b1} (5 nominal)	0.449	-0.445	2.2
	1.86×10^{-3}	-2.084×10^{-3}	479.9
	1.96×10^{-6}	$\pm j\,2.6\times10^{-4}$	479.9
Increased Q_{b2} (5 nominal)	2.21	-2.20	0.45
	8.07×10^{-3}	-1.83×10^{-3}	546
	7.46×10^{-6}	$\pm j\,2.6\times10^{-4}$	546
Increased Q_{a1} (33 nominal)	1.018	-1.008	0.99
	9.84×10^{-3}	-9.26×10^{-3}	108
	4.44×10^{-6}	-4.91×10^{-4}	2037
Increased Q_{a2} (33 nominal)	1.010	-1.003	0.997
	6.74×10^{-3}	-3.33×10^{-3}	300
	1.82×10^{-5}	$\pm j\,2.63\times10^{-3}$	300
Reduced Q_{b2} (0.01 nominal)	4.66×10^{-2}	-2.90×10^{-2}	34
	5.86×10^{-4}	-1.05×10^{-2}	95
Increased Q_{b1} (10 nominal)	1.004×10^{-6}	-6.78×10^{-3}	147

and the assumed noise densities, two of which have equal values. A dimensionally correct expression that also gives the right numerical value is discovered to be

$$k_1 \approx \sqrt{Q_{b2}/Q_{b1}} \tag{26}$$

This formula is in excellent agreement with the numerical results in Table 3 (except for the greatly reduced Q_{b2} case). The formula appears valid under the same conditions that give rise to the nested fast loop. A remarkable conclusion is that the first gain is optimized based only on the relative strengths of the two noise densities in the assumed altimeter error model.

One may derive additional useful formulas for the other gains as a function of the noise densities as follows. The explicit formula for the mean-square velocity error J as a function of the noise densities was given in Eq. (9). Assume that the nested fast loop conditions Eqs. (23) and (24) apply. Also assume that $k_2 \gg c$. Note that the numerical results indicated that the contribution of the term proportional to Q_{b1} was negligible. Assume that the gradient of this term with respect to k_2 and k_3 is also negligible. Delete this term from the analysis. An approximate formula for the cost (mean square velocity error) is then

$$2J \approx \frac{k_1}{k_2} Q_{a1} + \frac{k_1^2}{k_2 k_3} Q_{a2} + \left[\frac{k_2}{k_1} + \frac{k_3}{k_2} + \frac{2ck_1}{k_2} + \frac{c^2 k_1^2}{k_2 k_3}\right] Q_{b2} \tag{27}$$

Necessary conditions for a set of gains to be optimal include

$$\partial 2J/\partial k_2 = 0 \tag{28}$$

$$\partial 2J/\partial k_3 = 0 \tag{29}$$

Using Eq. (27) in Eq. (29) one obtains

$$k_3/k_1 \approx \sqrt{c^2 + Q_{a2}/Q_{b2}} \tag{30}$$

Similarly, using Eq. (27) in Eq. (28) and applying Eq. (30) one obtains

$$k_2/k_1 \approx [2c + Q_{a1}/Q_{b2} + 2\sqrt{c^2 + Q_{a2}/Q_{b2}}]^{1/2} \tag{31}$$

The preceding formulas for the gain ratios are in excellent agreement with the numerical results in Table 3, for all cases that have the nested fast loop.

An approximate formula for the location of the slower poles as a function of the noise densities may be derived by assuming $k_2' \approx k_2$ and by using Eqs. (30) and (31) in Eq. (25).

$$p_2, p_3 \approx -\tfrac{1}{2}[2c + Q_{a1}/Q_{b2} + 2\sqrt{c^2 + Q_{a2}/Q_{b2}}]^{1/2}$$
$$\pm \tfrac{1}{2}[2c + Q_{a1}/Q_{b2} - 2\sqrt{c^2 + Q_{a2}/Q_{b2}}]^{1/2} \tag{32}$$

This formula also is in excellent agreement with the numerical results.

An interesting observation supported by the computer results is that when the nested fast loop is optimal, the optimal second and third gain ratios (k_2/k_1 and k_3/k_1) as well as the optimal second and third pole locations are not a function of the assumed density of the short-correlation-time altimeter error. The computer results showed a factor of 5 increase in Q_{b1} producing a shift in the optimal time constant of less than 0.1%.

When the strength of the altimeter error random walk Q_{b2} is sufficiently large relative to the strength of the other sources of error, that is when

$$Q_{a1}/Q_{b2} \ll 2c \tag{33}$$

$$Q_{a2}/Q_{b2} \ll c^2 \tag{34}$$

then the optimal gain ratios and their associated pole locations and time constants are simply

$$k_2/k_1 \approx 2\sqrt{c} = 3.5 \times 10^{-3}\,\mathrm{s}^{-1} \tag{35}$$

Table 4 Error source initial values and statistics

Random walks $\dot{x} = w$		
Error source	Initial value	Noise spectral density N
X, Y (level) gyro drift rates	0.003 deg/h	$(0.003\ \mathrm{deg/h})^2/\mathrm{h}$
Z (azimuth) gyro drift rate	−0.295 deg/h	$(0.005\ \mathrm{deg/h})^2/\mathrm{h}$
X, Y (horizontal) accelerometer biases	50 μg	$(10\ \mu g)^2/\mathrm{h}$
Z (altitude) accelerometer bias	100 μg	$(10\ \mu g)^2/\mathrm{h}$
First-order Markov processes $\dot{x} = -\beta x + w$		$N_w = 2\beta\sigma^2$
Error source	Initial and 1σ value	Inverse correlation time, β
Barometric altimeter time-varying error	500 ft	$v/(250\ \mathrm{n.\ mi.})$
East deflection of gravity	26 μg	$v/(10\ \mathrm{n.\ mi.})$
North deflection of gravity	17 μg	$v/(10\ \mathrm{n.mi.})$
Gravity anomaly	35 μg	$v/(60\ \mathrm{n.\ mi.})$
Random constants $\dot{x} = 0$		
Error source		Initial value
G-sensitive gyro drift coefficients		0.3 deg/h/g
G^2-sensitive gyro drift coefficients		0.04 deg/h/g^2
X, Y gyro scale factor errors		300 ppm
Z gyro scale factor error		1000 ppm
Gyro input axis misalignments		±40 arc-sec
Accelerometer scale factor errors		150 ppm
X, Y accelerometer input axis misalignment about Z		±180 arc-sec
Other accelerometer input axis misalignments		±30 arc-sec
Barometric altimeter scale factor error		0.03
Coefficient of static pressure measurement error		1.54×10^{-4} ft/(ft/sec)^2
Barometric time delay		0.25 s

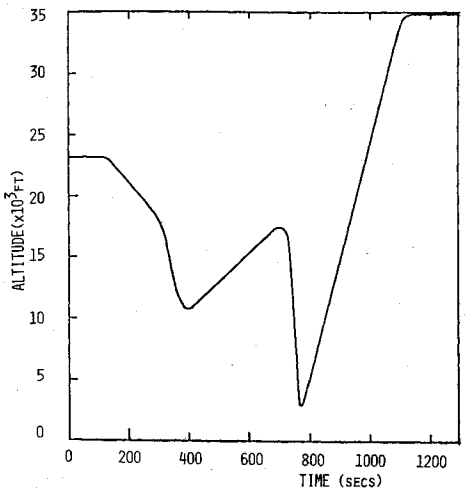

Fig. 2 Trajectory altitude history.

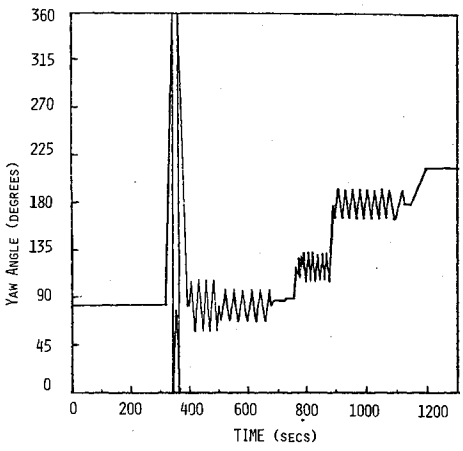

Fig. 3 Trajectory heading history.

$$k_3/k_1 \approx c = 3.07 \times 10^{-6}\,\mathrm{s}^{-2} \tag{36}$$

$$p_2, p_3 \approx -\sqrt{c} = -1.75 \times 10^{-3}\,\mathrm{s}^{-1} \tag{37}$$

$$\tau_2, \tau_3 \approx 1/\sqrt{c} = 571\ \mathrm{s} \tag{38}$$

These limiting results are a function only of the destabilizing gravity gradient c. Note that the nominal case, the increased Q_{b1} case, and especially the increased Q_{b2} case have computed results (Table 3) approaching this limiting case. An important conclusion is that even if the measured specific force is perfect (zero Q_{a1} and Q_{a2}), the feedback gain ratios k_2/k_1 and k_3/k_1 must be maintained at certain nonzero values to stabilize the vertical channel and to minimize the effect of the gravity computation error. These required values correspond to an upper limit on the optimal double pole time constant of 571 s.

When the strength of the acceleration short correlation error Q_{a1} is important in the sense that

$$2c + Q_{a1}/Q_{b2} \approx Q_{a1}/Q_{b2} \gg 2\sqrt{c^2 + Q_{a2}/Q_{b2}} \tag{39}$$

then the optimal gain ratio k_2/k_1 simplifies to

$$k_2/k_1 \approx \sqrt{Q_{a1}/Q_{b2}} \tag{40}$$

and Eq. (32) yields two real poles at

$$p_2 \approx -\sqrt{Q_{a1}/Q_{b2}} \tag{41}$$

$$p_3 \approx -\sqrt{(Q_{b2}/Q_{a1})c^2 + Q_{a2}/Q_{a1}} \tag{42}$$

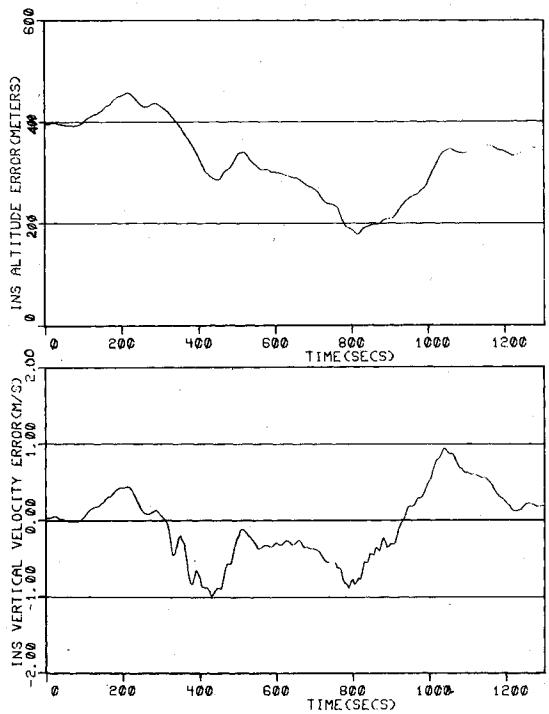

Fig. 4 Performance with baseline gains.

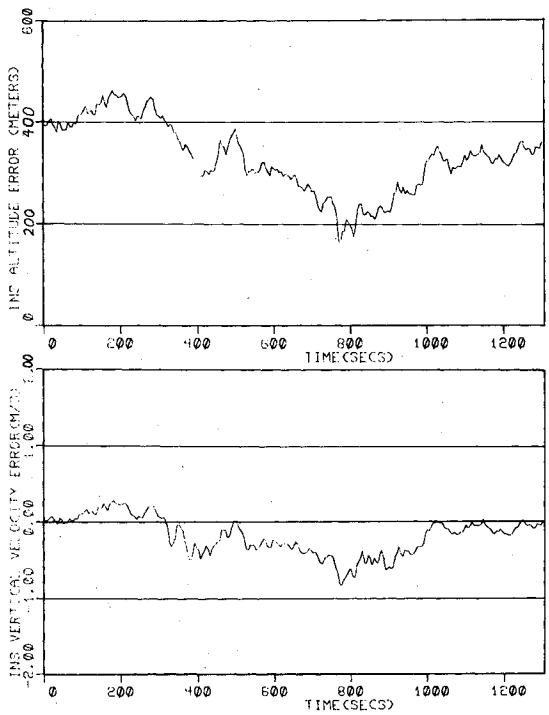

Fig. 5 Performance with optimized gains.

These formulas approximate computed results obtained in the increased Q_{a1} case (Table 3).

When the strength of the acceleration error random walk Q_{a2} is important in the sense that

$$2c + Q_{a1}/Q_{b2} \ll 2\sqrt{c^2 + Q_{a2}/Q_{b2}} \approx 2\sqrt{Q_{a2}/Q_{b2}} \tag{43}$$

then the optimal gain ratios are

$$k_2/k_1 \approx \sqrt{2}(Q_{a2}/Q_{b2})^{1/4} \tag{44}$$

$$k_3/k_1 \approx \sqrt{Q_{a2}/Q_{b2}} \tag{45}$$

and the associated pole locations are

$$p_2,p_3 \approx -(1/\sqrt{2})(Q_{a2}/Q_{b2})^{1/4}[1 \pm j] \quad (46)$$

These formulas approximate the computed residuals obtained in the increased Q_{a2} case (Table 3).

Simulated Performance

The vertical channel gains obtained by the optimization procedure have been evaluated using a time-domain three-channel simulation that includes detailed models for the sources of acceleration and altitude errors and that exhibits the dependence of these sources of error on the aircraft trajectory. Error sources included in the simulation are listed in Table 4. The aircraft trajectory simulated represents a F4 tactical mission profile. Figure 2 shows the altitude vs time. Figure 3 shows the heading vs time. This is a high dynamic trajectory. During the first descent the aircraft executes a "figure-eight" maneuver. During the remainder of the flight the aircraft is performing rapid zigzag evasive maneuvers while climbing and diving. In some of these maneuvers, maximum bank angles of 70 deg are used, with associated load factors of $3g$. One pull-up has a load factor of $5g$.

The vertical channel performance results with the baseline gains, Eq. (12), and with the optimized gains, Eq. (14), are exhibited in Figs. 4 and 5. The optimized gains do provide a lower level of vertical velocity error. A noticeable consequence of the fast ($\tau = 1$ s) loop around the indicated altitude is the increased noise content in the indicated altitude due to the baro-error fluctuations. This may be a disadvantage of the optimized gain set in some applications.

Conclusions

The fundamental assumptions underlying the results of this analysis are that the most important sources of error in the third-order vertical channel may be adequately modeled by random walks and white noises as presented earlier. If these assumptions are correct, then the following conclusions are obtained.

The most significant source of error in the vertical channel is the fluctuation in the altimeter bias (such as due to altimeter scale factor error and nonzero vertical velocity). The second most significant source of error is the short-correlation time acceleration error (such as due to specific force measurement error during a maneuver). Altimeter noise at the assumed level has negligible effect.

The optimal choice of the gain set is radically different from the baseline gain set, which provides a triple pole at $\tau = 100$ s. The optimal gains include a k_1 that is two orders-of-magnitude larger than that in the baseline set. The optimal value of k_1 is a function only of the relative strengths of the altimeter bias fluctuation and the altimeter noise. For the assumed relative strengths in the nominal case, the optimal gain value recommended is $k_1 = 1.0\ s^{-1}$. The optimal values for k_2 and k_3 are sensitive to the assumed numerical values for the noise densities. However, the optimal gain *ratios* k_2/k_1 and k_3/k_1 are relatively *in*sensitive to the assumed noises. The gain ratios recommended by the nominal optimal solution are $k_2/k_1 = 4.2\times10^{-3}\ s^{-1}$ and $k_3/k_1 = 4.4\times10^{-6}\ s^{-2}$. This choice of gains will place a fast pole at $\tau = 1$ s and a double pole at $\tau = 480$ s. This time constant of the optimal double poles is slower than the time constant of the baseline triple poles.

The optimal gains produce a significant performance improvement compared with the baseline case. The rms vertical velocity error is reduced 30%.

The recommended value for k_1 perhaps should be accepted with some degree of skepticism. However, the recommended values for the gain ratios k_2/k_1 and k_3/k_1 *can* be adopted with some confidence, because of their low sensitivity to the assumed noise values. The low sensitivity is a result of the gain ratios approaching a fundamental limit imposed by the destabilizing feedback of the gravity computation error.

If the short-correlation time acceleration error is more important than assumed in the nominal case, the optimal gain ratio k_2/k_1 increases and the optimal double pole splits into two real poles. On the other hand, if the acceleration error bias (such as due to accelerometer bias and gravity anomaly) is shifting more than assumed in the nominal case, both optimal gain ratios are increased and the optimal double pole splits into a complex conjugate pole pair.

A detailed baro-inertial error simulation has exhibited the reduced vertical velocity errors that can be obtained with the optimized gains. It provides confidence that the fundamental assumptions of the stochastic analysis are sound.

Because of the very long settling time associated with the recommended optimized gains, one should also implement a faster set of gains for use in the ground alignment mode.

References

[1] Draper, C.S., Wrigley, W., and Hovorka, J., *Inertial Guidance,* Pergamon Press, New York, 1960.

[2] McClure, C.L., *Theory of Inertial Guidance,* Prentice-Hall, Englewood Cliffs, N.J., 1960.

[3] Markey, W.R., *The Mechanics of Inertial Position and Heading Indication,* John Wiley & Sons, New York, 1961.

[4] Pitman, G.R., Jr. (ed), *Inertial Guidance,* John Wiley & Sons, New York, 1962, p. 41.

[5] O'Donnel, C.F., *Inertial Navigation, Analysis and Design,* McGraw-Hill, New York, 1964, pp. 35-36.

[6] Broxmeyer, C., *Inertial Navigation Systems,* McGraw-Hill, New York, 1964, p. 148.

[7] Farrell, J.L., *Integrated Aircraft Navigation,* Academic Press, New York, 1976, pp. 21-22.

[8] Kayton, M. and Fried, W.R., *Avionics Navigation Systems,* John Wiley & Sons, New York, 1969, pp. 317-319.

[9] Ausman, J.S., "GPS Bombing Demonstration Error Analysis," Litton Guidance & Control Systems Division presentation to General Dynamics Electronics Division, May 1976.

[10] Whalley, R., "Inertial Techniques in Height Measurement," *Journal of the Institute of Navigation,* Vol. 19, No. 1, 1966, pp. 61-67.

[11] Ausman, J.S. and Kouba, J., "Airborne Range Instrumentation System (ARIS)," Vol. II (Mechanization Equations), Litton Guidance and Control Systems Document No. 402029, Woodland Hills, Calif., Nov. 1972, pp. 25-28.

[12] Ausman, J.S., et al., "Close Air Support System (CLASS) F-4D Flight Test," Vol. I (Summary), Air Force Avionics Laboratory, Wright-Patterson Air Force Base, Ohio, TR-73-363, Sept. 1973, pp. 96-102.

[13] Blanchard, R.L., "A New Algorithm for Computing Inertial Altitude and Vertical Velocity," *IEEE Transactions on Aerospace and Electronic Systems,* Vol. AES-7, Nov. 1971, pp. 1143-1146.

[14] Newton, G.C., Gould, L.A., and Kaiser, J.N., *Analytic Design of Feedback Controls,* John Wiley & Sons, New York, 1961.

[15] Hooke, R. and Jeeves, T.A., "Direct Search Solution of Numerical and Statistical Problems," *Journal of the Association for Computing Machinery,* Vol. 8, April 1961, pp. 212-229.